SEMARAK ILMU PUBLISHING

Journal of Advanced Research in Fluid Mechanics and Thermal Sciences

Journal homepage:
https://semarakilmu.com.my/journals/index.php/fluid_mechanics_thermal_sciences/index
ISSN: 2289-7879

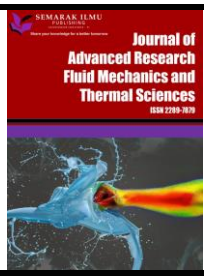

Thermo-Hydraulic Performance of Heated Tube with Twisted Delta Winglet Swirler Insert: A Numerical Simulation

At-Tasneem Mohd Amin[1,*], Wan Azmi Wan Hamzah[2], Mohd Azmi Ismail[3]

[1] Faculty of Mechanical and Automotive Engineering Technology, Universiti Malaysia Pahang, 26600 Pekan, Pahang, Malaysia
[2] Department of Mechanical Engineering, College of Engineering, Universiti Malaysia Pahang, 26300 Gambang, Pahang, Malaysia
[3] School of Mechanical Engineering, Universiti Sains Malaysia Engineering Campus, 14300 Nibong Tebal, Pulau Pinang, Malaysia

ARTICLE INFO

Article history:
Received 13 April 2022
Received in revised form 10 September 2022
Accepted 21 September 2022
Available online 12 October 2022

Keywords:
Convective heat transfer enhancement; friction factor; thermal-hydraulic performance; swirler; turbulator

ABSTRACT

Among the various methods for enhancing heat transfer in a heat exchanger, a passive method of inserting a continuous swirler inside a heated tube provides a secondary flow along the fluid that reduces the thickness of the thermal boundary layer, thus increasing the efficiency of convection heat transfer performance. The research's primary goal is to conserve energy, materials, and money by operating efficient heat exchanger equipment. However, the continuous swirler along the fluid flow creates a persistent obstruction, which amplifies the friction factor and increases the working fluid's energy loss. As a result, this research presented the twisted delta winglet swirler (TDWS), a new design of a decaying swirler that uses delta winglets twisted to 180° to produce a swirling flow along the tube. The swirler comprises four twisted delta winglets arranged in a circle with a diameter 6% smaller than the tube and a length of L/D=2.2. It was placed at the entrance to a heated tube test section with a diameter of 0.016 m and a length of L/D=93.75. The Reynolds Stress Model was used to simulate the flow domain with a water-ethylene glycol mixture was chosen as the working fluid. TDWS transformed the uniform inlet flow from potential energy to high kinetic energy, resulting in a high intensity of swirling flow downstream of the circular tube up to L/D=46.88 before decaying and reaching a steady state. Compared to other decaying swirlers, TDWS obtained one of the lowest relative friction factors, 1.36, with this flow. The maximum global relative Nusselt number increased by only 11% because this value considered the area where the flow reached a steady state. Since the TDWS is a decaying swirler, the thermal-hydraulic performance reached unity along the tube. However, the optimal performance of TDWS in the plain tube with a length of L/D=93.75 can be found if the dimension or geometric configuration of the TDWS is modified, or two or more TDWS may be placed in an array orientation.

1. Introduction

A vortex generator (VG) is a device that generates high vortex strength in a flow to create increased turbulence intensity, which improves heat transfer with less pressure loss. As shown in Figure 1, Skullong *et al.,* [1] construct a schematic diagram of four distinct types of VG that may be

* *Corresponding author.*
E-mail address: tasneem@ump.edu.my

https://doi.org/10.37934/arfmts.100.1.181200

connected or welded or cut and extruded to produce a delta/triangular or rectangular wing or winglet at various inclination angles, α with respect to the incoming flow. These VGs are extensively used in automobiles, aircraft, and ships to reduce drag and boost speed. At the same time, VG is widely used in a variety of mechanical devices, including gas turbine blades, heat engines, solar air heater ducts, solar chimneys, cooling tower, heat exchangers such as fin-tube heat exchangers, parallel flow heat exchangers, heat exchanger channels, corrugated-trapezoidal channel, tube bank and circular heat exchangers [2-14].

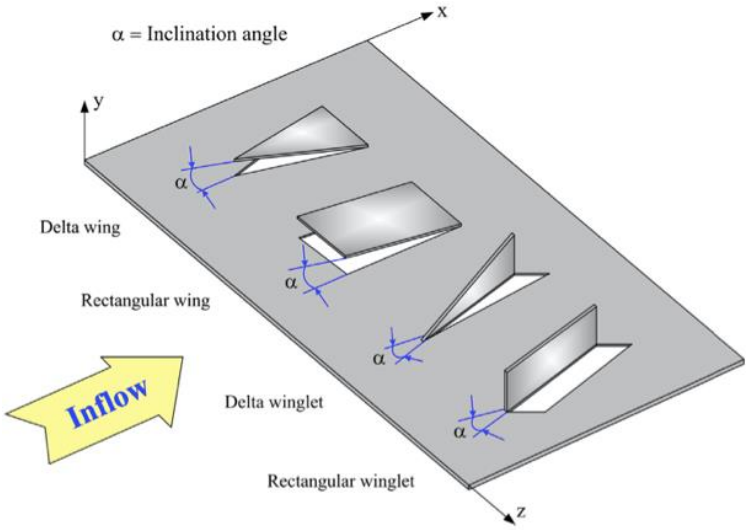

Fig. 1. Schematic diagram of different types of vortex generators [1]

In recent years, there has been an increase in the investigation of VG on plate inserts along circular heat exchangers. Figure 2 presents VG plates with various orientations examined for heat transfer enhancement in a heat exchanger. These VG plates were mounted along the pipe to provide a continuous mixing flow that periodically induces kinetic energy into turbulent flow. As a result, heat transfer improvement is persistent along the pipe. However, because the flow is constantly in contact with the surface of the VG along the tube, there will be continuous surface friction and blocking flow along the flow, resulting in a significant friction factor disadvantage. Promvonge and Skullong [15] placed a V-baffle VG at the edge of a flat plate to create counter-rotating vortices along the heated tube, enhancing heat transfer by minimising disturbance to the central core flow. This V-baffle VG improves heat transfer by 4.46 times more than a plain tube. Nonetheless, the peak relative friction factor was 18.25, remarkably higher than the plain tube. Skullong *et al.,* [1] used an inline array of perforated-delta winglets with a triangular hole punched on each winglet to reduce friction loss. The perforated-cross-tape (PW-XT) was employed to create streamwise vortex flows in the tube, reducing the thickness of the thermal boundary layer and increasing flow fluid mixing. Pourhedayat *et al.,* [16] discovered that longitudinal pitch has an extremum point, implying that the winglet should not be too close to the wall-side or central-side of the tube to limit friction inside the tube. Gururatana *et al.,* [17] mounted a modified NACA0024 VG at the top of a straight horizontal aluminium tape to improve flow circulation and longitudinal vortex within the tube. Although the VG angle of 120° provides the most significant improvement in Nusselt number, it also has an extremely high friction factor, which degrades the system's overall performance. Boonloi and Jedsadaratanachai [18] designed three different flow profiles using three different types of dual-inclined baffles (DIB). Because of the formation of a vortex and impinging streams, the DIB in a plain circular tube has a

higher heat transfer rate and thermal performance. The Nusselt number increased 17.46 times, whereas the friction factor increased 147.53 times more than the plain tube.

Promvonge and Skullong [15]

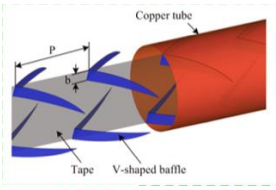

Pourhedayat *et al.,* [16]

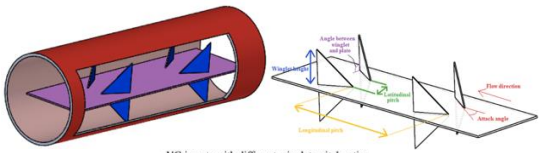

Khoshvaght-Aliabadi *et al.,* [19]

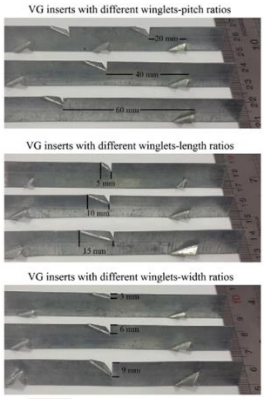

Boonloi and Jedsadaratanachai [18]

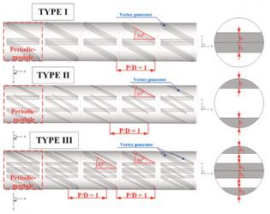

Gururatana *et al.,* [17]

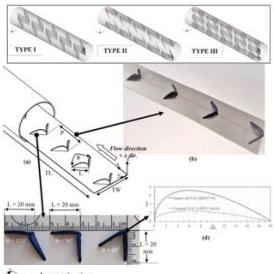

Wijayanta *et al.,* [20]

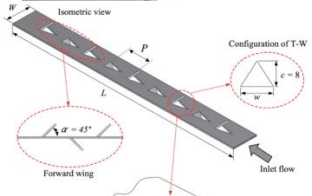

Skullong *et al.,* [1]

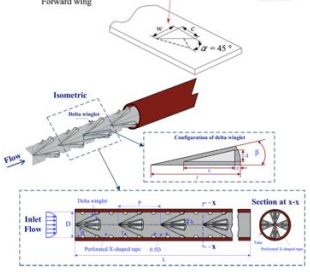

Fig. 2. Vortex Generator Geometries

This constant affixation of VG to the flat plate along the tube has been proven to significantly increase the friction factor along the pipe, necessitating substantial pumping capacity to propel the flow. The heat enhancement method was expected to increase system efficiency, so this finding was counter to that expectation. Thus, it was proposed to place the VG at the inlet rather than forming the vortex flow continuously throughout the flow, which would constantly drag the flow and create a very high friction factor. Numerous studies have been conducted specifically for this purpose. The winglet, vanes, or blades of a decaying flow swirler (also called a decaying turbulator or decaying swirl generator) are positioned within a circular tube at a specific twist angle to create a swirling flow. This device is installed at the inlet of the heat exchanger to induce swirling flow within the tube. The swirler's purpose is to separate the incoming axial flow into its component radial and tangential velocity so that the resulting swirling flow can continue unimpeded down the tube. Several swirler designs and their corresponding geometric parameters are shown in Figure 3 and Table 1.

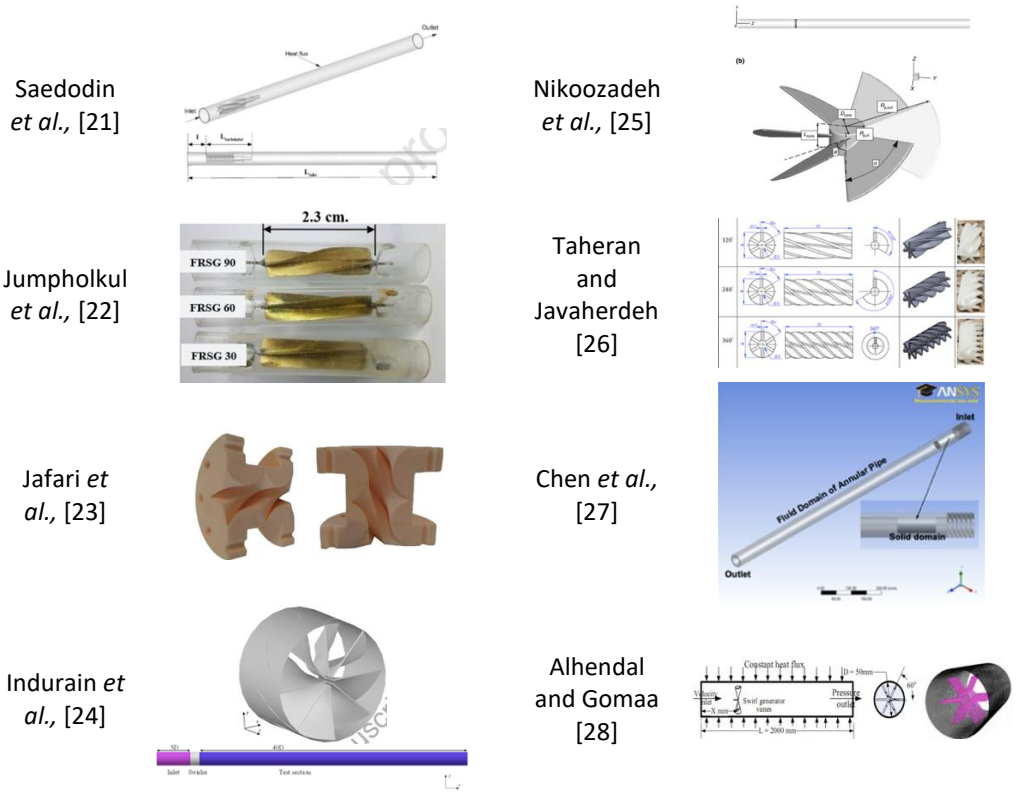

Fig. 3. Decaying swirlers

Table 1
Decaying Swirl Generators

Authors	Turbulator's category	Name of Vortex Generator	Swirler Dimensions	Location of swirler	Test Section	Flow Regime	No of Blade	Investigated Parameters	Enhancement of Nu	Increment of f	THP
Saedodin *et al.,* [21]	Twisted turbulator	Twisted turbulator	Length of turbulator, L/D=11.1	L/D=10.5	D=0.018m L/D=55.5	Re=10000 -45000	6	Different types of nanoparticles	7.93% (2 vol% SiO-water)	13.96% (SiO-water 2 col%)	1.063
Jumpholkul *et al.,* [22]	Twisted turbulator	Free rotating	L/D=3.2	L/D=0	D=0.0071 m L/D=281	Re=3500-13000	4	Inlet temp. (25°C, 30°C, 35°C,) Twisted angles (30°, 60°, 90°)	54.4% at 2 vol%, inlet T =35C, Re=10800.	9-20%	1.57-1.7
Jafari *et al.,* [23]	Twisted turbulator	Twisted tube with four-point star swirl generator	Diameter of turbulator is the same as diameter of the tube	L/D=0	L/D=3	Re=13246 -26492	4	Twist angle (T=90°, 180°, 270°, 360°)	75%	55%	1.54
Indurain *et al.,* [24]	Twisted turbulator	Axial guide vane swirler with profiling blades	L/D:0.5	L/D=5	D=0.4 m L/D=45.5	Re=10000 -200,000	8	Design of turbulator	1.57 at Re=10000.	2.9 at Re=200000	Higher than 1
Nikoozadeh *et al.,* [25]	Propeller turbulator	Propeller-type turbulator	D=0.053 m L/D=0.19	L/D=9	D=0.057 m L/D=34.7	Re=5000-30000)	6	Volume fractions and dia. of nanoparticles.	28%	68%	-
Xu *et al.,* [29]	Winglet turbulator	Winglet vortex generator	Delta winglet attached the inlet pipe wall	L/D=0	L/D=5.38	Re=6000-33000)	4	Angle β=0°, 15°, 30°, 45°) blockage ratios (B=0.1, 0.2, 0.3)	1.75 for Re=6000 and $\beta 45 - B0.3$.	320% with $\beta 45 - B0.3$	30%

A few different decaying flow swirler designs were introduced. The main goal of these approaches is to generate high-intensity swirl flow that can be sustained along the tube with minimal surface contact and device blockage. Saedodin *et al.,* [21], Jumpholkul *et al.,* [22], Taheran and Javaherdeh [26] and Chen *et al.,* [27] introduced twisted turbulators, Nikoozadeh *et al.,* [25] introduced a propeller turbulator, Indurain *et al.,* [24] and Alhendal and Gomaa [28] introduced profiled blades, and Jafari *et al.,* [23] introduced a twisted tube with four-point star swirl generator. All the study indicates the swirler's ability to improve heat transfer with less friction than continuous VG. Nusselt number and friction factor measurements, however, were taken in a manner analogous to that of a continuous VG, in which turbulence is continuously generated along the tube. On the other hand, the swirl flow is generated by the decaying flow swirler, which gradually diminishes as the flow continues down the tube after passing through the swirler. With a short tube, the average Nusselt number and friction factor will be high if the generated swirl flow is intense up until the outlet, resulting in a high relative Nusselt number. To the same extent, if the tube is too long, the average relative Nusselt number may be calculated to include the region where the swirl flow has vanished and the flow is at a steady state, resulting in a low relative Nusselt number. As a result, it is impossible to directly compare the reported values of the average relative Nusselt number for a decaying flow swirler.

For decaying swirlers, it is crucial that the dimensions of the swirler, the test section, and the location where the swirl flow is generated are specified in the literature. The reason is that each swirler produces varying levels of swirling intensity, which decays, dissipates, and eventually returns to the steady flow. For the heat transfer enhancement to be most effective, it is necessary to determine how far the swirling flow must travel before it settles into a steady state. However, each experiment has a unique test section. Jumpholkul *et al.,* [22] achieved a THP of 1.57 to 1.7 for a free-rotating swirl generator at Re greater than 7000 by using SiO2-water as the working fluid. The friction factor was marginally increased by 9 to 20% across all examined conditions. These results pertain to a test section with a length of L/D = 281. Contrarily, Jafari *et al.,* [23] provided evidence for the dimensionless length L/D=3. Using a twisted tube with a four-point star swirl generator and water/ethylene glycol working fluid, the highest THP of 1.54 was achieved at the lowest investigated Re of 12000 with the highest twisted angle of 360°. This swirler increased friction by up to 55% compared to a plain tube. Table 1 contains further examples.

Therefore, this work will thoroughly examine the production of swirl flow utilising a swirler inspired by a vortex generator. The swirler is known as the Twisted Delta Winglet Swirler (TDWS), and its design will be discussed in detail in the following section. The THP and survival of swirling flow along a plain horizontal tube will be presented. Previously, Xu *et al.,* [29] employed four delta winglets mounted on the inlet of the tube wall to produce turbulence downstream flow. The plain tube' test section has an L/D=5.38. The maximum THP of the delta winglets is 1.3 at an attach angle of 30° and a blockage angle of 0.1. At the same VG configuration, the friction factor percentage increased to 320%, and the highest relative Nusselt number was 1.75.

2. Methodology

2.1 Numerical Modelling

This simulation is a continuation of the studies carried out in ASHRAE Handbook [30]. The plain tube domain geometry is adapted from an experimental setup for forced convection heat transfer in a horizontal heated plain tube with a wire coiled insert. The Nusselt number was boosted by up to 254.4%. On the other hand, the friction factor was elevated by a maximum of 6.38 times that of the plain tube. Because of the high friction factor, the pump has to work harder to push the flow, increasing the pump's energy consumption. As a result, TDWS is introduced. The thermal-hydraulic

performance of TDWS will be numerically investigated using a commercial software ANSYS Fluent 2020. The water and ethylene glycol (W: EG) mixture was used as a working fluid at a 60% and 40% ratio. Table 2 shows the thermophysical properties of W: EG 60:40%.

Table 2
Thermophysical properties

Descriptions	Thermal conductivity, k [W/mK]	Density, ρ [kg/m^3]	Specific heat, C_p [J/kg.K]	Dynamic Viscosity, μ [Pa.s]
W:EG 60:40% [30]	0.4112	1055.832	0.002322	3498.6
Copper tube [31]	387.6	8978	381.0	-
Resin [32]	0.681	1229	-	-

The simulation is carried out on AMD Ryzen 9 3950X 16-Core CPU with 128 GB of Random Access Memory (RAM) and a processing speed of 3.49 GHz.

2.2 Computational Domain

Figure 4 illustrates the research's computational domain. The copper tube was divided into three parts for mesh generation purposes. The physical properties of the copper tube are listed in Table 2. The tube has a diameter of 0.016 m and a length of 1.5 m, or L/D=93.75. The TDWS is placed at the end of the entrance length at L/D=10. The 1.305 m long test section began after L/D=12.3.

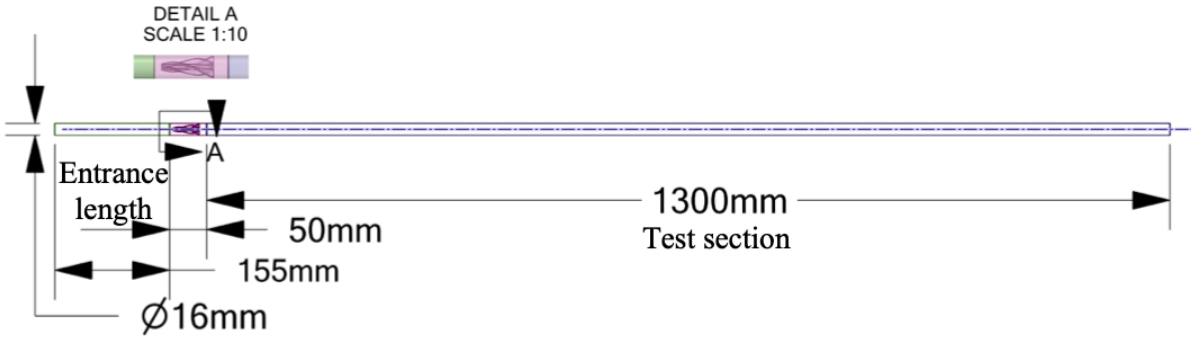

Fig. 4. Vortex Generator Geometries

2.3 Swirler Geometry

Figure 5 illustrates the geometry and dimensions of the TDWS. The TDWS was created by combining four delta winglets in a circle to create a vortex flow downstream of the tube. The design was realistic and capable of being 3D printed using resin elements and tested experimentally. Table 2 lists the physical properties of the resin. As a result, a 2 mm diameter hole was made in the centre of the TDWS to allow a small shaft holder to be put into the hole to retain the swirler inside the tube when it is physically tested in the laboratory. The swirler has a thickness of 0.98 mm to enable a minimum thickness of the wall elements to be printed using resin and to reduce blockage of incoming flow, which contributes to the high friction factor. The swirler's diameter is 15 mm, or 94% of the tube diameter, to provide a small region between the TDWS and the tube wall to generate boundary layers. The swirler's length is 35 mm, or L/D=2.2. The TDWS is twisted 180° to create a high-intensity swirl flow that can survive as far downstream as possible.

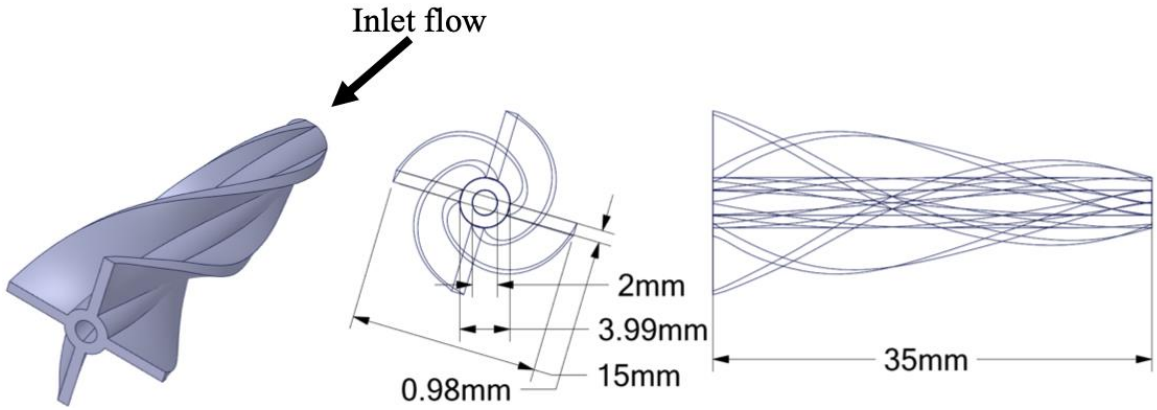

Fig. 5. TDWS Dimensions

2.4 Mesh Characterisation

As shown in Figure 6, the plain tube computational domain with TDWS was divided into three sections to generate multi-block meshes. The meshes were generated using Ansys Mesh Fluent. For simplicity, the structured mesh was constructed at the entrance length and test sections, whereas the unstructured mesh was generated at the TDWS section. The grid-independent test was performed on a plain tube with four distinct global mesh sizes: coarse, medium, fine, and superfine. The enhanced wall treatment was used to calculate the first layer thickness at y+=1. For all sections, the total inflation layer was set to 15 layers. The inflation growth rate was set at 1.15%.

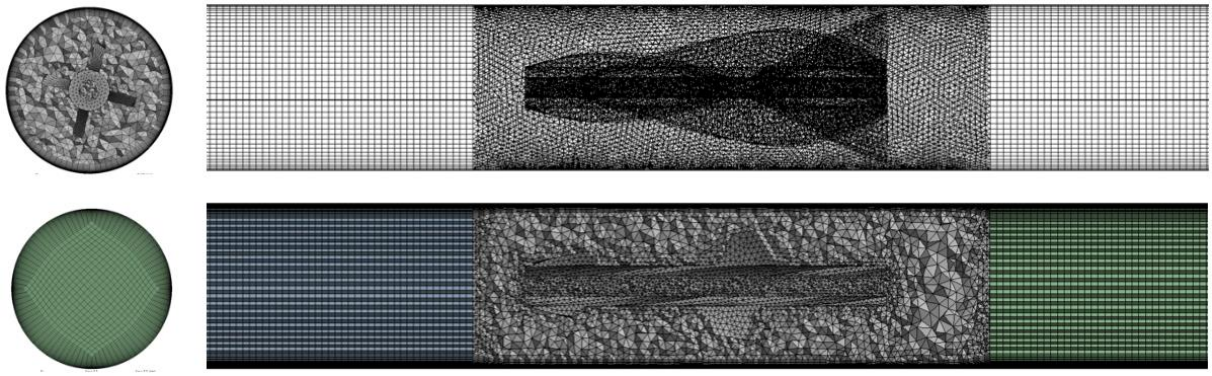

Fig. 6. Mesh Generation

2.5 Governing Equation

The simulation was carried out on a three-dimensional incompressible steady flow with Reynolds numbers, Re ranging from 4583 to 35000. The governing equations for continuity, Reynolds Averaged Navier-Stokes (RANS), and energy are as follows.

Continuity equation

$$\frac{\partial(\rho u_i)}{\partial x_i} = 0, i = 1, 2, 3 \quad (1)$$

Reynolds-average momentum equations

$$\frac{\partial(\rho u_i u_j)}{\partial x_j} = -\frac{\partial P}{\partial x_i} + \frac{\partial}{\partial x_j}\left[\mu\left(\frac{\partial u_i}{\partial x_j} + \frac{\partial u_j}{\partial x_i}\right)\right], j = 1, 2, 3 \quad (2)$$

Energy equation

$$\frac{\partial}{\partial x_i}\left(\rho u_i C_p T - k\frac{\partial T}{\partial x_i}\right) = 0 \quad (3)$$

The Reynolds stress model (RSM) was used to solve transport equations, incorporating individual Reynolds stresses $< u_i' u_i' >$ to predict the turbulence characteristics downstream of the TDWS. Because the RSM is more refined than any other Reynolds Average Navier-Stokes (RANS) model, Yan *et al.,* [33] also used RSM for the numerical evaluation of a decaying multi-lobed swirl generator in a plain horizontal tube.

2.6 Boundary Condition

The boundary condition of a heated tube with TDWS inserts is demonstrated in Figure 7. A uniform inlet velocity computed from Re is provided as an inlet condition. The W: EG 60: 40% inlet temperature was kept at room temperature (29 °C) to transfer forced convection heat between the flowing fluid and the heated wall. To measure the pressure difference along the straight tube, the outlet is adjusted to have a gauge pressure equal to zero. The horizontal copper plain tube was subjected to a constant heat flux of 7957 W/m^2. TDWS wall was set to an adiabatic wall condition. The tube and TDWS were adjusted to a non-slip state with a velocity at the wall equal to zero.

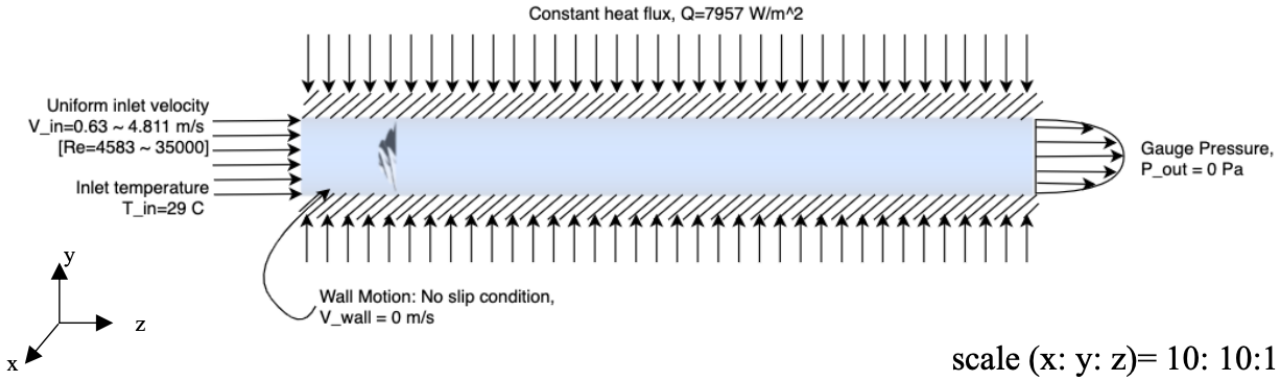

Fig. 7. Boundary condition

2.7 Grid Independent Test

The grid independent test runs through a verification and validation process to confirm that the numerical setup is correct, with the correct boundary conditions, turbulence model, and parameter values, before comparing the results to valid correlations. The verification test was carried out for four mesh size levels by measuring the flow's maximum velocity inside the plain tube at Re=10136. The dimensionless parameter of Nusselt number for the plain tube was then validated by comparing it to the Dittus and Boelter [34] and Gnielinski [35] equations as follows

Dittus-Boelter equation

$$Nu_D = 0.023 Re_D^{\frac{4}{5}} Pr^n \text{ for } n = 0.3\ (T_s < T_m), n = 0.4\ (T_s > T_m) \quad (4)$$

Gnielinski equation

$$Nu_G = \frac{\left(\frac{f}{8}\right)(Re_D - 1000)Pr}{1 + 12.7\left(\frac{f}{8}\right)^{\frac{1}{2}}\left(Pr^{\frac{2}{3}} - 1\right)} \quad (5)$$

where

Re_D is Reynolds number calculated from the inlet flow, and
Pr is Prandtl number for W:EG 60:40%.

2.8 Parameter Definition

The thermal-hydraulic performance (THP) of any turbulence generation device (continuous and decaying) implanted within the tube is typically evaluated to identify the ratio of the relative heat transfer coefficient, Nu_{rel} to the penalty of the friction loss in the flow, f_{rel}. In certain publications, it is also referred to as the thermal enhancement factor (TEF), thermal efficiency (Eff), or performance evaluation criterion (PEC).

This paper will compare the effect of the presence of TDWS inside the plain tube to the plain tube. The comparison between friction factor and Nusselt number on a local and global scale will be thoroughly examined. Finally, Thermal-hydraulic Performance (THP) is calculated to reflect the heat transfer enhancement under a particular pumping power, utilising the total thermal-hydraulic performance of the tube with a swirler insert. The following parameters are examined

<u>Local parameters</u>

Darcy friction factor

$$f_{local} = dP_{local} \frac{D}{L} \frac{2}{\rho {V_{in}}^2} \quad (6)$$

Forced convection heat transfer coefficient

$$h_{local} = \frac{\dot{q}}{(T_s - T_b)} \quad (7)$$

Local Nusselt number

$$Nu_{local} = \frac{h_{local} D}{k} \quad (8)$$

Global parameters

Darcy friction factor

$$f = dP_L \frac{D}{L} \frac{2}{\rho {V_{in}}^2} \quad (9)$$

Forced convection heat transfer coefficient

$$h = \frac{\dot{q}}{(T_s - T_b)} \quad (10)$$

Global Nusselt number

$$Nu = \frac{hD}{k} \quad (11)$$

T_s and T_b were calculated by taking the average of both data along the tube.

Relative parameters

Relative friction factor

$$f_{rel} = \frac{f_{TDWS}}{f_{PT}} \quad (12)$$

Relative Nusselt number

$$Nu_{rel} = \frac{Nu_{TDWS}}{Nu_{PT}} \quad (13)$$

Thermal hydraulic performance

$$THP = \frac{Nu_{rel}}{{f_{rel}}^{\frac{1}{3}}} \quad (14)$$

where

dP is pressure drop between the specified location and outlet of the tube flow
$\dot{q}$ is a constant heat flux that applied along the plain tube
T_s is wall surface temperature
$T_b$is bulk temperature of the flow, measured at the centre core fluid
k is thermal conductivity of W: EG 60:40%

Nu_{TDWS} is the Nusselt number of the flow when the swirl generator was inserted in the tube Nu_{PT} is the Nusselt number of the flow of the plain tube.

3. Result

3.1 Grid Independent Test

A verification test was performed on a heated plain tube at maximum velocity for four levels of mesh ranging from coarse to superfine. The number of elements ranged from 303912 to 9238775, as indicated in Table 3.

Table 3
Verification Test

Mesh Number	Mesh Size [mm]	Number of Layer Inflation	Growth rate	Number of elements	Velocity Max [m/s]
Course	2	15	1.15	303912	1.702
Medium	0.8	15	1.15	2123136	1.728
Fine	0.6	15	1.15	3888486	1.732
Superfine	0.4	15	1.15	9238775	1.732

The maximum velocity result remained consistent after the mesh size was reduced from fine to superfine mesh with a mesh increase of up to 5 million elements, as presented in Figure 8. As a result, a fine mesh configuration was chosen for the validation procedure. The validation process for the range of Re for Nusselt numbers was then carried out by comparing the data with correlation equations. The results reveal that the simulation results are in good agreement between the two correlations, with an average relative error of 3% for the Dittus-Boelter equation and 0.2% for the Gnielinski equation.

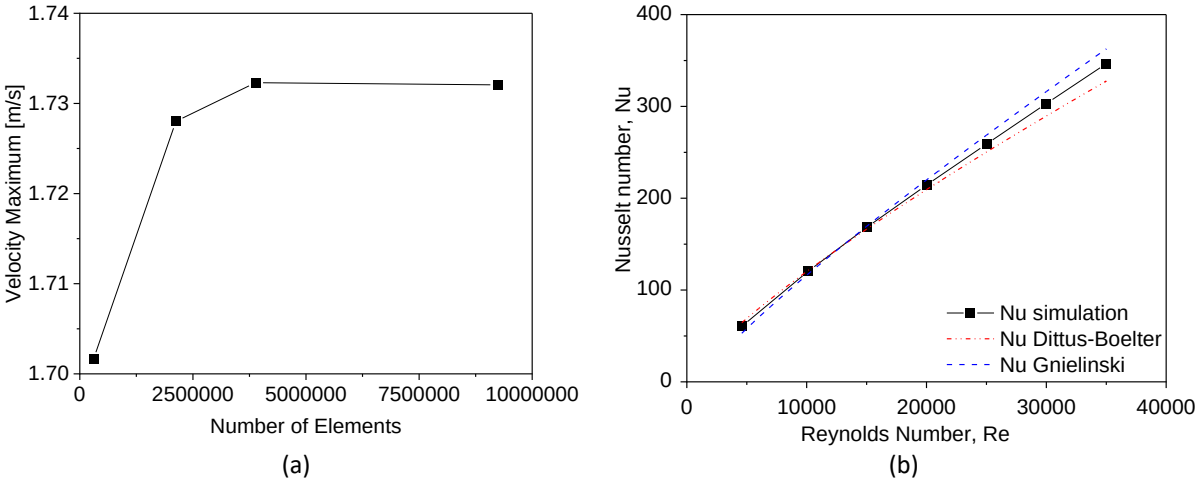

Fig. 8. Grid Independent Test (a) Verification test (b) Validation test

3.2 Flow Visualisations

Figure 9 exhibits the swirling flow turbulence intensity and the axial and circumferential velocity contours created by TDWS in the heated tube. The x- and y-axis are enlarged to make it easier to see the flow through the z-axis along the tube. The red and yellow contours show high swirling flow intensity, while the green and blue contours represent low swirling flow intensity. To obtain a clear vision of the flow inside the tube, the opposite colour contour to the turbulence intensity was employed for axial and circumferential velocity.

The turbulence intensity is essentially non-existent at the flow's inlet. As it passes through the TDWS, the high intensity of the turbulence flow is generated downstream. The swirling flow gradually decays as the flow moves towards the tube's outlet. The swirling flow virtually vanished after L/D=46.88. To get a closer look at what happened inside the tube, the section plane of turbulence intensity and the velocity circumferential along the tube were visualised. Consider the cross-section flow at L/D=23.44; both turbulence intensity and circumferential velocity are lowest at the viscous layer and considerably increase as the flow passes through the logarithmic and buffer layers. Nonetheless, the turbulence intensity and circumferential velocity steadily decrease as it moves further toward the core region. This contour is due to the drag effect of the TDWS structure blockage, which prevents the swirling flow from generating in the core region. The drag effect gradually decreases as the flow moves downstream. The swirling intensity from the outer layer of the flow is gathered to generate a higher flow intensity in the centre region. As the flow travelled further downstream, the turbulence energy steadily decreased, and therefore the turbulence intensity lessened. On the other hand, the axial velocity is highest at the input of the flow, is distorted after passing through the TDWS, and is restored as it moves downstream toward the tube's outlet. The axial velocity profile along the tube shows that it was minimum near the wall and gradually increased towards the central cores of the tube flow.

3.3 Local Parameter

One hundred points of wall and centerline temperature, as well as pressure, were measured along the tube to examine the local friction factor, f_{local} and local Nusselt number, Nu_{local}, and their relative value with and without the presence of TDWS.

Figure 10(a) compared the f_{local} along the plain tube and the tube with the TDWS insert. In general, for both with and without TDWS inserts, the f_{local} is maximum at a low Re and decreases as the Re increases. The f_{local} of the plain tube is constant along its length for all Re. Nevertheless, when the TDWS was placed at L/D=10, the f_{local} is dramatically increased along the entrance length. As shown in Figure 10(b), the relative local friction factor, $f_{local,rel}$ increases to near 1.29 for Re=35000 at L/D=0 and reaches a maximum of 1.41 for Re=15000 at L/D=9.5, just before the flow enters the TCWS region at L/D=10. As the flow enters the TCWS, the friction factor drops drastically until it reaches a minimum of 0.63 at L/D=14.2 at the highest Re=35000. This trend is because the flow velocity in this region is greatly enhanced since the incoming flow approaching the TCWS wall is forced to bend toward a twisted angle, causing the flow to become chaotic between the winglets before exiting the TCWS region. As a result, the pressure in this region drops, and so does the friction factor. As the flow leaves the trailing edge of TDWS, it encounters the drag effect, where the pressure is minimum behind the TCWS and gradually recovers as it flows downstream at L/D=46.88.

On the other hand, Figure 10(c) shows the local Nusselt number, Nu_{local} for the plain tube and the plain tube with the presence of TDWS at L/D=10. The Nu_{local} is minimum along the tube at the lowest investigated Re. As the Re increased, so did the Nu_{local}. As displayed at the entrance length of the tube, the Nu_{local} in the plain tube experiences the instant increment of the Nu_{local} as the inlet fluid experiences the heat supplied at the wall. The flow becomes fully developed after L/D=10, with the Nu_{local} essentially constant until the tube outlet. With the presence of TDWS in the tube, the Nu_{local} multiplies until it reaches the highest relative local Nusselt number, $Nu_{local,rel}$ with 3.08 at L/D=13.26, which is near the trailing edge of the TDWS at the lowest investigated Re, as shown in Figure 10(d). As the flow travels downstream, the Nu_{local} fluctuates in response to the swirling flow patterns, gradually decreasing as it moves further down the tube. TDWS inside the tube causes a high intensity of swirling flow, thinning the boundary layer near the wall. As a result, the heat from the

high temperature at the wall where the constant heat flux was supplied was quickly transferred to the lower temperature at the core region. Simultaneously, the random movement of the particles inside the working fluid collides, translating and twisting between one another, allowing heat to be transferred faster than at lower Re. The graph of $Nu_{local,rel}$ clearly demonstrates that the flow steadily decays as it flows downstream along the tube towards the tube's outlet. The swirling flow decays as the kinetic energy generated at the trailing edge of the TDWS is slowly dissipated due to friction between the fluid particles and the walls until it returns to a steady state.

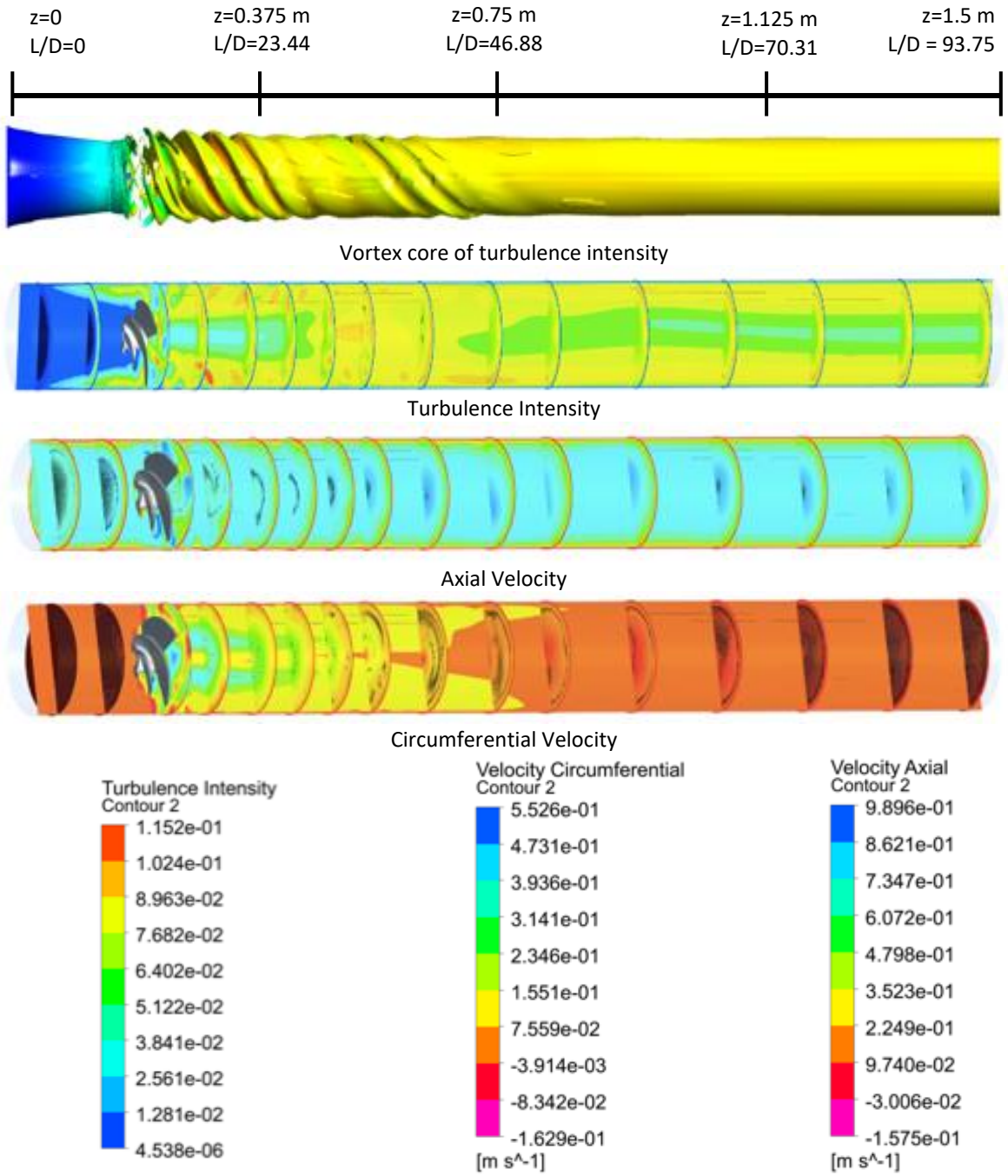

Fig. 9. Flow visualization (scale x: y: z= 10: 10: 1)

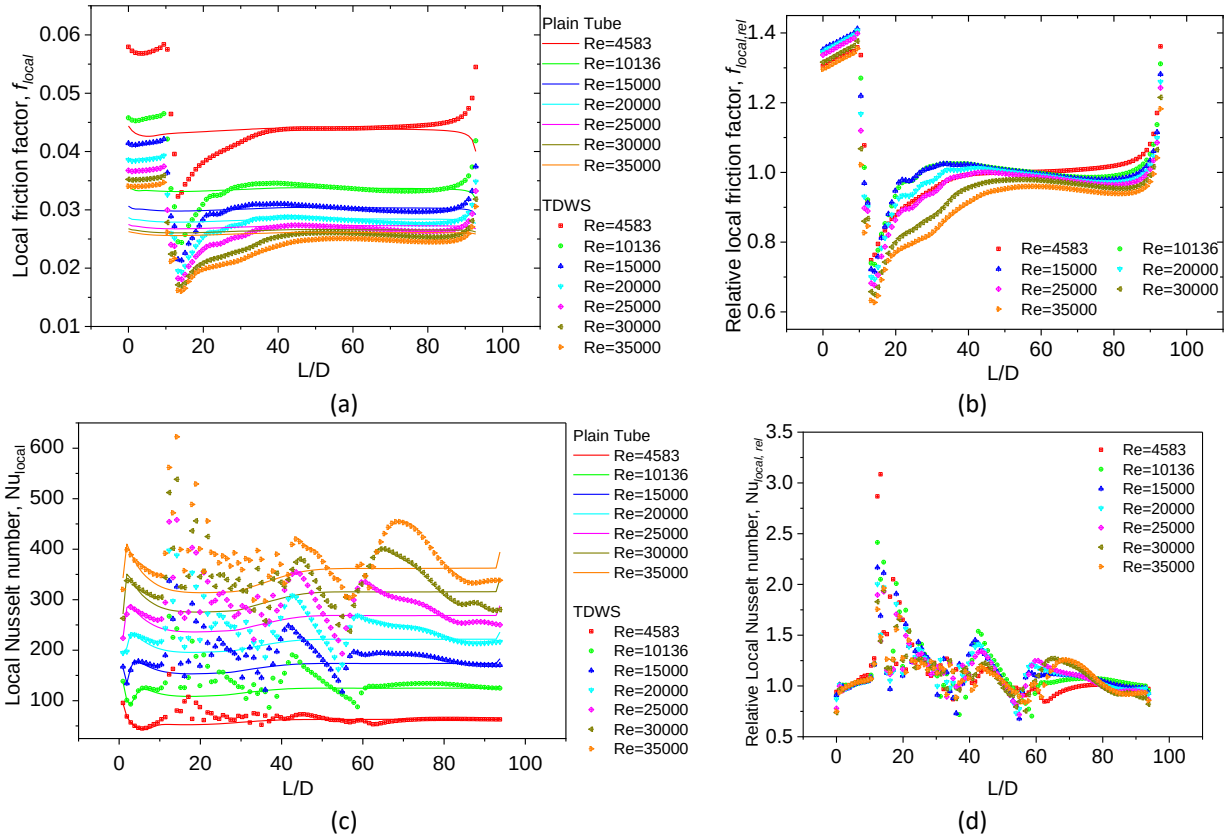

Fig. 10. Local parameters (a) Local friction factor (b) Relative local friction factor (c) Local Nusselt number (d) Relative local Nusselt number

3.4 Global Parameter

The pressure difference at the inlet and outlet of the tube was used to derive the global parameter for the friction factor. The global parameter of the Nusselt number was obtained by taking the average of both wall surface and centre core temperatures along a 1.5 m tube to compute the forced convection heat transfer, which was then used to calculate the Nusselt number. Figure 11(a) displays the flow's global friction factor and Nusselt number with and without TCWS insert. The friction factor is represented by the left vertical axis, while the right vertical axis represents the Nusselt number. The friction factor decreases significantly as the Re increases, while the Nusselt number increases linearly. The presence of TDWS in the tube raises the friction factor and Nusselt number above the value for the plain tube. The left vertical axis in Figure 11(b) represents the relative friction factor, f_{rel} and the right vertical axis represents the relative Nusselt number, Nu_{rel}. As the Re increases from 4583 to 35000, both parameters exhibit a negative quadratic relationship. The maximum f_{rel} was obtained at Re=15000 with a value of 1.36. Aside from Saedodin *et al.,* [21], the circular tube with TDWS insert produced the lowest f_{rel} of any decaying swirler in Table 1. However, since this simulation was performed in a tube twice as long as that used by Saedodin *et al.,* [21] and the location of the decaying swirler was similar, the f_{rel} for TDWS is considered to be reasonably consistent with this literature. On the other hand, the maximum Nu_{rel} was obtained at Re=20000 with a value of 1.11. This value is lower than that of the other swirlers.

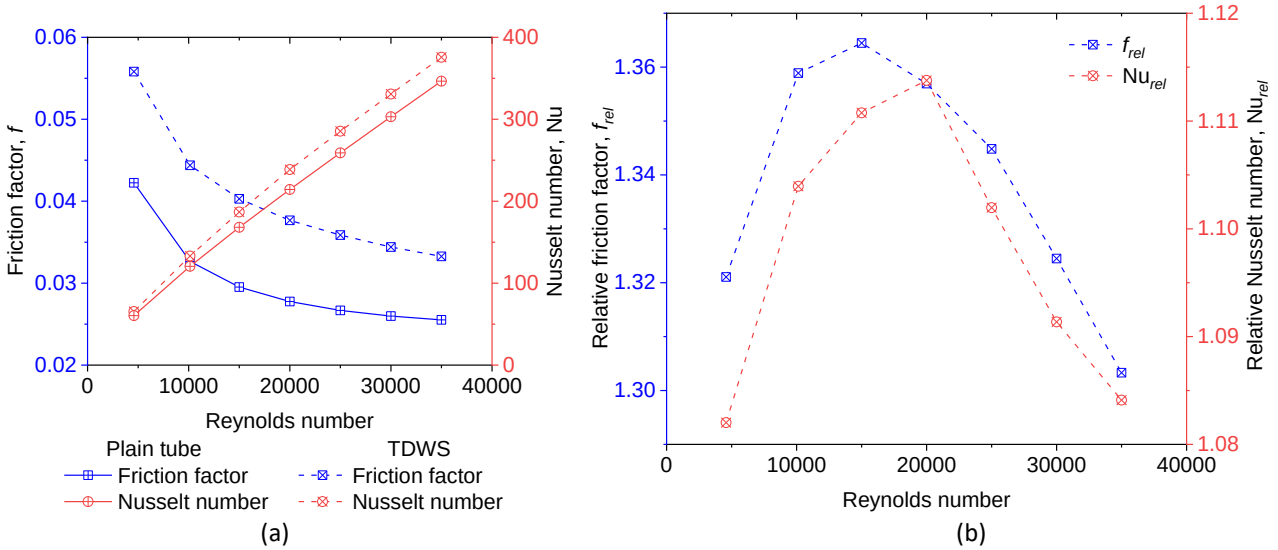

Fig. 11. Global parameters (a) Friction factor and Nusselt number Relative friction factor and relative Nusselt number

To better understand TDWS's global Nusselt number performance, the Nu_{local} along the tube with TDWS inserts with the maximum global Nusselt number was examined. Table 4 shows the maximum and minimum Nu_{local} at each swirling cycle from the TDWS trailing edge to the tube outlet. The Nu_{local} steadily decays as the flow travels along the tube. At the same time, the Nu_{local} fluctuated below 1.0 due to the mixing flow of fluid with high and low temperatures. The Nu_{local} eventually recovered to a steady state after L/D=81 for this Re. The global Nusselt number is low because it was computed by taking the average of Nusselt numbers along the tube while taking the influence of fluctuation and decaying flow into account.

Table 4
Maximum and minimum Nu_{local} at Re=20000

Swirling flow travels (L/D)	Maximum Nu_{local}	Minimum Nu_{local}
12.3 – 20.0	2.00	1.05
21.0 – 40.0	1.54	0.88
41.0 – 60.0	1.41	0.73
61.0 – 80.0	1.17	1.01
81.0 – 93.7	1.0	0.91

3.5 Thermal-Hydraulic Performance

After determining the friction factor and Nusselt number, the thermal-hydraulic performance was evaluated locally and globally, as shown in Figure 12. As illustrated in Figure 12(a), the local thermal-hydraulic performance, THP_{local} follows a similar trend to Nu_{local}. As the value is observed down the tube, it fluctuates and decays. At the trailing edge of TDWS at the lowest investigated Re, the maximum THP local of 3.4 was obtained. On the other hand, Figure 12(b) represents the global thermal-hydraulic performance, THP, of TDWS inside the circular tube. The graph reveals that the THP has reached its maximum at unity at all Re examined, except for the lowest Re with 0.988. These findings show that, while utilising the same pumping power, the TDWS increased the forced convection heat transfer of a circular horizontal tube with L/D=93.75 by up to 11% at Re=15000 and 20000.

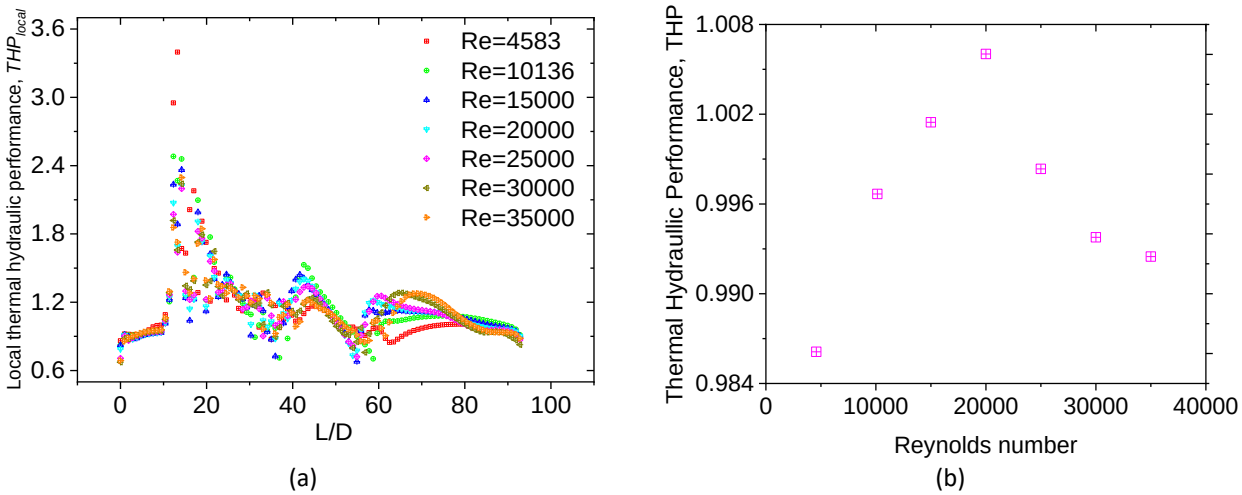

Fig. 12. Thermal-hydraulic performance (THP) (a) Local THP (b) Global THP

To assess the endurance of the swirling flow along the L/D=93.75 tube, the average THP_{local} is computed by sections. Table 5 compares the average of THP_{local} in each section for Re=20000, where the maximum global THP was reached. This data revealed that if TDWS is utilised for the tube length up to L/D=20 or 0.32 m, the THP of the circular heat exchanger with TDWS insert at the exact location, the global THP will improve up to 60%. This value drops as the tube length extends. As a result, depending on the THP performance desired, TDWS can be applied.

Table 5
Average THP_{local}

Swirling flow travels (L/D)	Tube length [m]	Average THP_{local}
12.3 – 20.0	0.32	1.60
12.3 – 40.0	0.64	1.32
12.3 – 60.0	0.96	1.24
12.3 – 80.0	1.28	1.21
12.3 – 93.7	1.50	1.00

All the results presented show that TDWS can improve the efficiency of a circular heat exchanger. Nonetheless, because the TDWS is a decaying swirler, the swirler's performance fluctuates, decays, and stabilises after L/D=81. The dimension and geometry configuration of the TDWS require minor changes to improve the turbulence intensity and survivability of the swirling flow, hence delaying the decaying rate of the swirling flow. Otherwise, to maintain the current dimension and design configuration, two or more TDWSs in array orientation may be introduced to maintain their good performance.

4. Conclusions

A new decaying swirler design named the twisted delta winglet swirler (TDWS) was numerically evaluated to minimise the friction factor while using the same pumping power to maximise heat transfer efficiency in a circular heat exchanger system. TDWS comprises four delta winglets twisted together in a circle to create a swirling flow down the tube. It was positioned at the entrance to the test section to reduce blocking along with the flow. W: EG with a 60: 40% ratio was used as a working fluid at room temperature, with Reynolds numbers ranging from 4583 to 35000. Constant heat flux was supplied to the tube to conduct a forced convection heat transfer analysis on the circular heat exchanger system. The maximum relative local and global friction factors are 1.41 and 1.36,

respectively, as are the maximum relative local and global Nusselt numbers of 3.08 and 1.11. As a result, the local and global thermal-hydraulic performance (THP) is 3.4 and unity, respectively. Because the TDWS is a decaying swirler, the swirling flow is intense as it passes through the swirler; it fluctuates, decays, and returns to a steady state as it flows downstream the tube. Consequently, the global parameters are lower than the continuous swirlers described in the literature. TDWS can be adjusted by optimising its dimensions or geometry configuration or arranging it in tandem to fully utilise the high-intensity zone of swirling flow.

Acknowledgement
The authors would like to thank Universiti Malaysia Pahang for financial support under Internal Research grant RDU190385.

References

[1] Skullong, Sompol, Pongjet Promvonge, Chinaruk Thianpong, and Nuthvipa Jayranaiwachira. "Thermal behaviors in a round tube equipped with quadruple perforated-delta-winglet pairs." *Applied Thermal Engineering* 115 (2017): 229-243. https://doi.org/10.1016/j.applthermaleng.2016.12.082

[2] Zhao, Zhiqi, Lei Luo, Dandan Qiu, Songtao Wang, Zhongqi Wang, and Bengt Sundén. "On the topology of vortex structures and heat transfer of a gas turbine blade internal tip with different arrangement of delta-winglet vortex generators." *International Journal of Thermal Sciences* 160 (2021): 106676. https://doi.org/10.1016/j.ijthermalsci.2020.106676

[3] Xie, Pengyong, and Xiaobing Zhang. "The influence of active dynamic control flow vortexes on enhancing convective heat transfer." *International Journal of Thermal Sciences* 168 (2021): 107058. https://doi.org/10.1016/j.ijthermalsci.2021.107058

[4] Promvonge, Pongjet, Pitak Promthaisong, and Sompol Skullong. "Numerical heat transfer in a solar air heater duct with punched delta-winglet vortex generators." *Case Studies in Thermal Engineering* 26 (2021): 101088. https://doi.org/10.1016/j.csite.2021.101088

[5] Oh, Yeongtaek, and Kuisoon Kim. "Effects of position and geometry of curved vortex generators on fin-tube heat-exchanger performance characteristics." *Applied Thermal Engineering* 189 (2021): 116736. https://doi.org/10.1016/j.applthermaleng.2021.116736

[6] Sheikhnejad, Yahya, and Seyed Abdolreza Gandjalikhan Nassab. "Enhancement of solar chimney performance by passive vortex generator." *Renewable Energy* 169 (2021): 437-450. https://doi.org/10.1016/j.renene.2021.01.026

[7] Mugisidi, Dan, Oktarina Heriyani, Pancatatva Hesti Gunawan, and Dwi Apriani. "Performance Improvement of a Forced Draught Cooling Tower Using a Vortex Generator." *CFD Letters* 13, no. 1 (2021): 45-57. https://doi.org/10.37934/cfdl.13.1.4557

[8] Tepe, Ahmet Ümit. "Heat transfer enhancement of fin-tube heat exchangers using punched triangular ramp vortex generator on the fin surface." *International Journal of Heat and Mass Transfer* 174 (2021): 121326. https://doi.org/10.1016/j.ijheatmasstransfer.2021.121326

[9] Zhao, Zhiqi, Lei Luo, Dandan Qiu, Zhongqi Wang, and Bengt Sundén. "On the solar air heater thermal enhancement and flow topology using differently shaped ribs combined with delta-winglet vortex generators." *Energy* 224 (2021): 119944. https://doi.org/10.1016/j.energy.2021.119944

[10] Carpio, José, and Alvaro Valencia. "Heat transfer enhancement through longitudinal vortex generators in compact heat exchangers with flat tubes." *International Communications in Heat and Mass Transfer* 120 (2021): 105035. https://doi.org/10.1016/j.icheatmasstransfer.2020.105035

[11] Yu, Chulin, Youqiang Wang, Haiqing Zhang, Min Zeng, Bingjun Gao, and Zhou Fang. "Numerical investigation on turbulent thermal performance of parallel flow heat exchanger with a novel polyhedral longitudinal vortex generator in shell side." *International Journal of Thermal Sciences* 166 (2021): 106962. https://doi.org/10.1016/j.ijthermalsci.2021.106962

[12] Han, Zhimin, Zhiming Xu, and Hongwei Qu. "Parametric study of the particulate fouling characteristics of vortex generators in a heat exchanger." *Applied Thermal Engineering* 167 (2020): 114735. https://doi.org/10.1016/j.applthermaleng.2019.114735

[13] Nfawa, Sadeq Rashid, Abd Rahim Abu Talib, Siti Ujila Masuri, Adi Azriff Basri, and Hasril Hasini. "Heat transfer enhancement in a corrugated-trapezoidal channel using winglet vortex generators." *CFD Letters* 11, no. 10 (2019): 69-80.

[14] Lin, Chou Aw, Fatimah Al-Zahrah Mohd Sa'at, Fadhilah Shikh Anuar, Muhammad Firdaus Sukri, Mohd Zaid Akop, and Zainuddin Abdul Manan. "Heat Transfer Across Tube Banks With a Passive Control Vortex Generator in Steady One-Directional and Oscillatory Flows." *CFD Letters* 13, no. 1 (2021): 1-18. https://doi.org/10.37934/cfdl.13.1.118

[15] Promvonge, Pongjet, and Sompol Skullong. "Enhanced thermal performance in tubular heat exchanger contained with V-shaped baffles." *Applied Thermal Engineering* 185 (2021): 116307. https://doi.org/10.1016/j.applthermaleng.2020.116307

[16] Pourhedayat, Samira, Seyed Mehdi Pesteei, Hamed Ebrahimi Ghalinghie, Mehran Hashemian, and Muhammad Aqeel Ashraf. "Thermal-exergetic behavior of triangular vortex generators through the cylindrical tubes." *International Journal of Heat and Mass Transfer* 151 (2020): 119406. https://doi.org/10.1016/j.ijheatmasstransfer.2020.119406

[17] Gururatana, Suabsakul, Rotchana Prapainop, Sathaporn Chuepeng, and Sompol Skullong. "Development of heat transfer performance in tubular heat exchanger with improved NACA0024 vortex generator." *Case Studies in Thermal Engineering* 26 (2021): 101166. https://doi.org/10.1016/j.csite.2021.101166

[18] Boonloi, Amnart, and Withada Jedsadaratanachai. "Numerical assessments of flow pattern and heat transfer profile for the round tube equipped with different configurations of the dual-inclined baffle." *Case Studies in Thermal Engineering* 27 (2021): 101242. https://doi.org/10.1016/j.csite.2021.101242

[19] Khoshvaght-Aliabadi, M., M. H. Akbari, and F. Hormozi. "An empirical study on vortex-generator insert fitted in tubular heat exchangers with dilute Cu-water nanofluid flow." *Chinese Journal of Chemical Engineering* 24, no. 6 (2016): 728-736. https://doi.org/10.1016/j.cjche.2016.01.014

[20] Wijayanta, Agung Tri, Indri Yaningsih, Wibawa Endra Juwana, Muhammad Aziz, and Takahiko Miyazaki. "Effect of wing-pitch ratio of double-sided delta-wing tape insert on the improvement of convective heat transfer." *International Journal of Thermal Sciences* 151 (2020): 106261. https://doi.org/10.1016/j.ijthermalsci.2020.106261

[21] Saedodin, Seyfolah, Mohammad Zaboli, and Seyed Hadi Rostamian. "Effect of twisted turbulator and various metal oxide nanofluids on the thermal performance of a straight tube: Numerical study based on experimental data." *Chemical Engineering and Processing-Process Intensification* 158 (2020): 108106. https://doi.org/10.1016/j.cep.2020.108106

[22] Jumpholkul, Chaiwat, Lazarus Godson Asirvatham, Ahmet Selim Dalkılıç, Omid Mahian, Ho Seon Ahn, Dong-Wook Jerng, and Somchai Wongwises. "Experimental investigation of the heat transfer and pressure drop characteristics of SiO_2/water nanofluids flowing through a circular tube equipped with free rotating swirl generators." *Heat and Mass Transfer* 56, no. 5 (2020): 1613-1626. https://doi.org/10.1007/s00231-019-02782-z

[23] Jafari, Mohammad, Amir Farajollahi, and Heshmatollah Gazori. "The experimental investigation concerning the heat transfer enhancement via a four-point star swirl generator in the presence of water-ethylene glycol mixtures." *Journal of Thermal Analysis and Calorimetry* 144, no. 1 (2021): 167-178. https://doi.org/10.1007/s10973-020-09408-1

[24] Indurain, Bruce, François Beaubert, Sylvain Lalot, and David Uystepruyst. "Computational Fluid Dynamics Investigation of the Thermal Performances of a Swirler with Profiled Blades." *Heat Transfer Engineering* 42, no. 17 (2021): 1452-1472. https://doi.org/10.1080/01457632.2020.1800271

[25] Nikoozadeh, A., A. Behzadmehr, and S. Payan. "Numerical investigation of turbulent heat transfer enhancement using combined propeller-type turbulator and nanofluid in a circular tube." *Journal of Thermal Analysis and Calorimetry* 140, no. 3 (2020): 1029-1044. https://doi.org/10.1007/s10973-019-08578-x

[26] Taheran, Ehsan, and Kourosh Javaherdeh. "Experimental investigation on the effect of inlet swirl generator on heat transfer and pressure drop of non-Newtonian nanofluid." *Applied Thermal Engineering* 147 (2019): 551-561. https://doi.org/10.1016/j.applthermaleng.2018.07.142

[27] Chen, Baiman, Kelvin Ho, Hanmin Xiao, Yousif A. Abakr, and Andy Chan. "The effects of swirling decaying flow towards pipe entry length and heat transfer in an annular pipe." *International Journal of Heat and Mass Transfer* 123 (2018): 668-677. https://doi.org/10.1016/j.ijheatmasstransfer.2017.12.160

[28] Alhendal, Yousuf, and Abdalla Gomaa. "Three Dimensional CFD Modeling of Turbulent Flow Through Circular Tube Using Swirl Generator Vanes at Different Positions." *International Journal of Mechanical and Production Engineering* 5, no. 6 (2017): 106-11.

[29] Xu, Y., M. D. Islam, and N. Kharoua. "Numerical study of winglets vortex generator effects on thermal performance in a circular pipe." *International Journal of Thermal Sciences* 112 (2017): 304-317. https://doi.org/10.1016/j.ijthermalsci.2016.10.015

[30] ASHRAE Handbook. "ASHRAE Handbook-Fundamental: SI Editions." *American Society of Heating, Refrigerating and Air-Conditioning Engineers. Inc.: Atlanta, GA, USA* (2009).

[31] Perry, Robert H., and Don W. Green. *Perry's chemical engineers' handbook. 7th ed*. McGraw-Hill Professional, 1997.

[32] Hu, Guang, Zhi Cao, Michael Hopkins, John G. Lyons, Margaret Brennan-Fournet, and Declan M. Devine. "Nanofillers can be used to enhance the thermal conductivity of commercially available SLA resins." *Procedia Manufacturing* 38 (2019): 1236-1243. https://doi.org/10.1016/j.promfg.2020.01.215

[33] Yan, Tie, Jingyu Qu, Xiaofeng Sun, Ye Chen, Qiaobo Hu, and Wei Li. "Numerical evaluation on the decaying swirling flow in a multi-lobed swirl generator." *Engineering Applications of Computational Fluid Mechanics* 14, no. 1 (2020): 1198-1214. https://doi.org/10.1080/19942060.2020.1816494

[34] Dittus, F. W., and L. M. K. Boelter. "Heat transfer in automobile radiators of the tubular type." *International Communications in Heat and Mass Transfer* 12, no. 1 (1985): 3-22. https://doi.org/10.1016/0735-1933(85)90003-X

[35] Gnielinski, Volker. "On heat transfer in tubes." *International Journal of Heat and Mass Transfer* 63 (2013): 134-140. https://doi.org/10.1016/j.ijheatmasstransfer.2013.04.015